Experimental study of phase relations in the U–Ti–Al ternary system

Chantal Moussa, Mathieu Pasturel, Bertrand Stepnik, Olivier Tougait

Experimental study of phase relations in the U-Ti-Al ternary system.

Chantal MOUSSA[1], Mathieu PASTUREL[1], Bertrand STEPNIK[2], Olivier TOUGAIT[1]*

[1] Institut des Sciences Chimiques de Rennes, équipe Chimie du Solide et Matériaux, UMR6226, CNRS-Université de Rennes 1, Avenue du Général Leclerc, 35042 Rennes – France

[2] AREVA/CERCA, 10 Rue Juliette Récamier, 69006 Lyon – France

***Corresponding Author:**
O. Tougait
ISCR/CSM
263 avenue du Général Leclerc
35042 Rennes Cedex
France
tougait@univ-rennes1.fr

Abstract

The phase relations in the ternary U-Ti-Al system were established for the whole concentration range for two temperatures, 923 K and 1123 K. They were derived from quenched samples annealed at 1123 K for about 500 hours and at 923 K for about 720 hours using X-ray powder diffraction, scanning electron microscopy and energy dispersive spectroscopic analysis. Only one ternary phase, the Al-rich compound, UTi_2Al_{20}, was found. It forms by a peritectic reaction at 1365(5)K, and remains stable at least down to 923K. Based on single-crystal structure refinements, it was confirmed that it adopts the $CeCr_2Al_{20}$ structure type (cubic, $Fm\bar{3}d$, n°227) with lattice parameter at room temperature, a = 14.634(1) Å. Unlike most of the isotypic aluminides, UTi_2Al_{20} should be regarded as a line compound. At 1123 K, the isothermal section is characterized by the extended homogeneity ranges due to mutual exchange between U and Ti and between Ti and Al in the unary phases, whereas at 923 K, the mutual solubility between U and Ti was found null. Regarding the binary phases, only in the Laves phase, UAl_2 (cubic-C15, $MgCu_2$-type) such solubilities were observed with limits of about 2 at.% of U by Ti and 5.5 at.% of Al by Ti, at 1123 K. For the other binary compounds, the solubility of the third component was found negligible at both temperatures.

Keywords : A. intermetallics**; B.** crystal chemistry**; B.** phase-transformation; **F**. differential thermal analysis; **F**. electron microscopy scanning; **F.** X-ray diffraction.

1. Introduction

The magnetic properties of intermetallic compounds containing uranium and a 3*d*-transition metal are of particular interest because the extended 5*f* wave function could lead to strong hybridization with 4*s*, 4*p* or 3*d* wave functions of the neighboring atoms, giving rise to exotic phenomena [1]. However, in case of strengthening hybridization, the delocalization of both the *f*- and *d* –electrons causes a large reduction of the magnetic moments down to the cancelation as observed e.g. UCo_2 [2] and $U_{10}Ni_{13}$ [3]. Along the 3*d* row of the periodic table, the increase of the electronegativity from the left to the right goes with a narrowing of the bandwidth [4, 5]. Therefore, moderate hybridization between 5*f* and 3*d* orbitals is rather expected with early transition metals than late ones. In this respect, ternary uranium and titanium compounds provide engaging examples of magnetic ordering with strong anisotropy as encountered in U_3TiGe_5 [6] and U_3TiSb_5 [7] or with enhancement of the Curie temperature as found in the pseudo-binary compounds $UFe_{2-x}Ti_x$ [8]. To date, only one ternary compound is reported in the U-Ti-Al system, UTi_2Al_{20} [9]. It crystallizes in the cubic symmetry with the $CeCr_2Al_{20}$ structure type. The study of its electronic properties revealed Pauli paramagnetism [10]. The exploration of the U-Ti-Al system could result in the discovery of new ternary phases.

In addition, binary systems which exhibit large solubility domains in γU (*bcc* form, W-type) are of interest for research reactor fuel conversion from High Enriched Uranium (HEU) to Low Enriched Uranium (LEU). In these dispersed fuels, the fissile material is embedded in an Al-matrix and then clad into Al foils in order to frame a thin fuel plate. Up to now, the most promising alloy has been γU(Mo). However, to overcome the close interaction between the fuel meat and the Al-matrix [11], alloying with other gamma stabilizers such as Ti was considered [12, 13]. In this respect, the phase equilibria and compatibility within the ternary U-Ti-Al system can provide valuable information for the fabrication process and the in-pile behavior.

Since (i) no information is published on the phase relations in the U-Ti-Al system, (ii) systematic investigation in the whole concentration range is a valuable method for identifying new phases and (iii) phase equilibria can supply helpful knowledge about the used properties of γU based alloys in an Al matrix, we have undertaken the assessment of the U-Ti-Al subsolidus phase relations for two temperatures, 923 K and 1123 K. The present paper proposes both isothermal sections, along with a reinvestigation of the crystal structure of UTi_2Al_{20} regarding the Ti/Al substitution mechanism and its thermodynamic properties.

2. Experimental section

For each of the two annealing temperatures, samples were prepared, covering the entire ternary composition domain. High purity metals, uranium pieces (99.8 wt.%), titanium sponge (99.99 wt.%) and aluminum rods (99.999 wt.%) were arc-melted and heat-treated under partial atmosphere of Ar at 1123 K for about 500 hours or at 923 K for about 720 hours. After the heat-treatment, the samples were quenched in air. Samples taken from both as-cast and heat-treated buttons were ground into powder for X-ray diffraction experiments and embedded into a resin and polished down to a 1 µm grain size diamond paste for microscopic analyses, which were mainly performed by Scanning Electron Microscopy combined with Energy Dispersive Spectroscopy (SEM-EDS).

Single crystals of UTi_2Al_{20}, suitable for crystal structure determination, were obtained by the Al flux method, according to the procedure used for growing UMo_2Al_{20} crystals [14]. The diffraction intensities were collected at room temperature on a Nonius Kappa CCD four-circle diffractometer working with Mo Kα radiation (λ = 0.71073 Å). The integration and the reduction of redundant reflections of the different data sets as well as the cell refinements were performed using DENZO software [15]. Numerical absorption corrections were made with the use of the program ANALYTICAL [16]. The structural model was taken from the isotypic $CeCr_2Al_{20}$-type of compounds [9, 10, 14]. All the structure refinements and Fourier syntheses were made with the help of SHELXL-14 [17].

DTA analyses were performed on some samples using a Setaram Labsys device at temperatures up to 1873 K, with heating and cooling rates in the range of 5-20 K per minute.

3 Results and discussion

3.1 The binary boundary systems

The binary boundary systems U-Ti, U-Al and Ti-Al were mainly accepted from the critical assessment of the binary alloy phase diagrams by Massalski [18], despite the fact that two more recent thermodynamic assessments of the Ti-Al system were available [19, 20] giving almost identical information at our working temperatures. Table 1 summarizes the main crystallographic data and phase stability of the unary and binary phases bounding the U-Ti-Al system.

In agreement with the literature data (mainly Massalski, [18]) the following binary phases were found stable at 1123 K and/or at 923 K: UAl_2 (Cubic, $Fd\bar{3}m$), UAl_3 (cubic, $Pm\bar{3}m$), UAl_4

(orthorhombic, *Imma*, stable only at 923K), U_2Ti (hexagonal, *P*6/*mmm*) Ti_3Al (cubic, *Pm-3n*), TiAl (tetragonal, *P4/mmm*), $TiAl_2$ (tetragonal, $I4_1/amd$) and $TiAl_3$ (hexagonal, $P6_3/mmc$). Our analyses of their elemental compositions show that the three intermediate phases of the U-Al system, U_2Ti and $TiAl_3$ are stoichiometric compounds. The homogeneity range of $TiAl_2$ which doesn't exceed 1 at.%, is within the experimental error of the EDS technique and was considered in our experimental study as a line compound in agreement with [19,20]. On the opposite, the homogeneity ranges of TiAl and Ti_3Al were confirmed for both temperatures (see Table 1).

3.2 Phase relations at 923 K

The results of our experimental investigation of the samples annealed at 923 K for about 720 hours are shown in Figure 1. X-ray powder diffraction was used to determine the crystallographic phases present whereas the EDS analyses give the elemental composition of the respective phases. Selected measured compositions defining two-phase fields and three-phase fields are compiled in Table 2. They were obtained by averaging the values of at least three EDS analyzed points, from different regions of the sample, with a tolerance of 2 at.% on each element. Some X-ray diffraction patterns and microstructures featuring three-phase fields are illustrated in Figure 2 and Figure 3, for samples with composition 11.32U-7.55Ti-81.13Al and 40U-40Ti-20Al, respectively.

The isothermal section is mainly characterized by tie-lines between binary phases. With the exception of UAl_2 (Laves phase C15), negligible solubility of the third component in the binary phases can be deduced from our measurements. For αU, αTi, Ti_3Al and TiAl, our EDS measurements confirm the solubility ranges reported in the literature (Table 2). The solubility of Ti in UAl_2 reaches 5 at.% at 923 K. The U composition remains close to 33.3 at.% which indicates an Al/Ti substitution. The lattice parameter of this pseudo binary phase, refined over three different samples, converges to a = 7.763(4) Å, for the maximum substitution rate, which is almost identical to the value a = 7.769(3) Å, that we refined for the pure binary compound (UAl_2). This small difference between these lattice parameters results from the moderate rate substitution and from the close metallic radii for Al and Ti (r_{Al} = 1.432 Å and r_{Ti} = 1.462 Å) [35]. The ternary compound UTi_2Al_{20} is the only intermediate phase in this ternary system.

Eleven three-phase and five two-phase fields compose the isothermal section at 923 K. The Al-rich part comprises the unique ternary compound, UTi_2Al_{20}, which is in equilibrium with Al, UAl_4, UAl_3 and $TiAl_3$. X-ray powder analyses confirm their reported structural type. As illustrated in Table 2, no solubility of U or Ti in Al was detected. In agreement with the previous reports

[9,10], UTi_2Al_{20} crystallizes with the $CeCr_2Al_{20}$ type with no evident solubility range around the stoichiometric composition at 923 K. Two two-phase fields are separated by the ternary extension of $UAl_{2-x}Ti_x$ ($0<x<0.15(2)$), one with αU, whose limit was evaluated with a sample of composition 38U-5Ti5-57Al, and a second one, with TiAl phase, which covers the whole homogeneity domain of both phases. EDS analyses of samples within the UAl_2-UAl_3-$TiAl_3$ three-phase field give a Ti content below 1 at.% in UAl_2 which is the limit of accuracy of EDS method, as illustrated by the 24U-5Ti-71Al sample. Thus, the possible U/Ti substitution in UAl_2 was evaluated to be negligible. Therefore, the UAl_2 pure binary composition is in equilibrium with UAl_3, $TiAl_3$ and $TiAl_2$. No solubility of U could be detected in TiAl.

Regarding the Al-poor part of the triangle, no solubility of Al or Ti was detected in U metal, which was found to crystallize in its low temperature allotropic form (α-form, orthorhombic, *Cmcm*). A large three-phase field is defined between αU-$UAl_{2-x}Ti_x$(x = 0.15(2)-TiAl as illustrated by the 50U-20Ti-30Al sample. In addition to the two-phase field with the ternary extension of $UAl_{2-x}Ti_x$, αU delimits a second two-phase field with Ti_3Al, but limited to the range 66-73 at.% Ti, as illustrated by the 40U-40Ti-20Al and 65U-30Ti-5Al samples. The remaining part of the solubility domain of Ti_3Al (73-78 at.% Ti) delimits a two phase field with U_2Ti. Finally U_2Ti delimits a two-phase field with the homogeneity domain of αTi (0-12.5 at.% Al), as illustrated by the 10U-80Ti-10Al sample. The hexagonal structure of αTi (Mg-type, hexagonal, $P6_3/mmc$) was confirmed by X-ray diffraction.

3.3 Phase relations at 1123 K

The isothermal section at 1123 K was studied in the whole concentration range with special attention to the vicinity of the U-Ti axis, where most of the changes with the previous temperature are observed. The phase equilibria are shown graphically in Figure 4. They were established from analyses of X-ray diffraction patterns and EDS measurements of samples annealed at 1123 K for 500 hours. Selected elemental compositions determined in various two-phase and three phase fields are summarized in Table 3.

Literature data of unary and binary phases at 1123 K compared to those at 923 K, revealed a small liquid phase in the Al-rich corner, with a ternary extension limited to less than 1 at.% Ti and less than 2 at.% U. Regarding the Ti-Al binary system, the same four intermediate phases exist, only small variations of the homogeneity ranges about TiAl, Ti_3Al and αTi occur. For the U-Al binary system, only UAl_3 and UAl_2 are stable at 1123 K and a small solid solution limited to 2 at.% Al in γU develops. Most of the changes occur in the U-Ti system, with the formation of

two solid solutions, (i) one based on γU dissolving up to 15 at.% Ti, (ii) another one based on βTi in the range 2-34 at.% U, which is separated from αTi by a small two-phase field. The intermediate phase U_2Ti is still stable at 1123 K. Most of these thermodynamic features regarding the unary and binary systems are listed in Table1.

In the Al-rich corner of the isotherm, the small liquid phase was estimated according to the literature data. The phase equilibria with the melt were not determined precisely. However, EDS analyses of 8U-4Ti-88Al and 2U-9Ti-89Al samples support the phase composition expected for such solidified melt (dotted line in Figure 4). The solubility of the third component in the various binary phases was examined, no ternary extension was found for UAl_3, $TiAl_3$, $TiAl_2$, TiAl and Ti_3Al as illustrated by 2U-63Ti-30Al, 4U-48Ti-48Al and 38U-5Ti-57Al samples (Table 3). The only significant ternary extension was found for the UAl_2 Laves phases. From the EDS analysis of the 33U-22Ti-45Al, 40U-10Ti-50Al and 50U-20Ti-50Al samples, the limit of Ti/Al substitution can be evaluated at 5.5 at.% Ti. A small U/Ti substitution of about 2 at.% Ti measured for the 16.67U-16.67Ti-66.66Al sample suggests that the ternary extension of UAl_2 has a triangle shape. This ternary extension based on UAl_2 divides two two-phase fields, (i) one ending at the γU solid solution, (ii) the second one ending with TiAl. The two-phase and three phase fields involving the U-corner converge to a composition of $U_{96}Ti_2Al_2$ which adopts the high temperature form of U (γ-form, *bcc*). Despite the fact that this cubic structure could not remain stable down to room temperature, the microstructure of this phase, observed on several samples, clearly evidences the eutectoid transformation $\gamma U \rightarrow \alpha U + U_2Ti$, as illustrated in Figure 5. This image obtained for a sample with composition 70U-28Ti-2Al, comprises three phases, Ti_3Al (black areas), U_2Ti (medium-grey areas) and U (light-grey areas). The light-grey areas show small dendritic grains trapped into a matrix, which is a typical morphology of a eutectoid decomposition (lamellar morphology). The U-corner defines a γU solid solution with a triangular shape and delimited by compositions of $U_{98}Al_2$ and $U_{84}Ti_{16}$, in line with our experimental results. These results are in good agreement with the value expected from the literature data (see table 1). The two-phase field is delimited between γU [$U_{96}Ti_2Al_2$ – $U_{84}Ti_{16}$] and Ti_3Al, (64-72.5 at.% Ti). The phase Ti_3Al with composition 72.5-78 at.% Ti defines a two-phase field with U_2Ti.

In the Ti-rich corner, the X-ray diffraction patterns confirm the cubic symmetry indicating a large solid solution based on βTi. It was drawn as a straight line between $Ti_{98}U_2$, $Ti_{66}U_{34}$ and an average ternary composition based on the EDS analysis of the samples 16U-80Ti-4Al and 10U-80Ti-10Al. the tie-lines between βTi and αTi could not be determined experimentally.

3.4 Crystal structure refinements of the UTi_2Al_{20} ternary phases

Unlike most of the other ternary phases crystallizing with the $CeCr_2Al_{20}$ type [9, 14], no solubility range seems to exist for UTi_2Al_{20}. This observation is based on EDS analyses which have an accuracy of about 1 at.%. Therefore, in order to determine more accurately a possible Ti/Al substitution mechanism, crystal structure refinements of UTi_2Al_{20} have been carried out using single crystal X-ray diffraction data. Single crystals were obtained by the Al flux method. The conditions for crystal data collection are gathered in Table 4, the refined atomic positions are given in Table 5.

The refinements of the occupancy parameters were performed for the 5 non-equivalent positions, resulting in negligible deviation. Therefore, the chemical formula thus deduced from the refinement of this single crystal prepared with a large excess of aluminum yields UTi_2Al_{20}, which combined with the EDS results, indicates a line-compound.

DTA measurements coupled with XRD analysis of a sample initially composed of UTi_2Al_{20} only, suggest a peritertic formation at 1365(5) K according to the reaction $UAl_3 + TiAl_3 + L \rightarrow UTi_2Al_{20}$.

4 Conclusion

Phase relations in the U-Ti-Al ternary system established from quenched samples heat-treated at 923 K and 1123 K have been constructed. Our results indicate that the previously reported compound, UTi_2Al_{20} is the only intermediate phase to form in this ternary system. It forms according to a peritectic reaction at 1365(5) K from $UAl_3 + TiAl_3$ and liquid. At 923 K, the solubility of Ti in UAl_3 and in UAl_4 is very low or negligible, whereas the solubility of Ti is up to 5 at.% in UAl_2 which remains a cubic $MgCu_2$-type structure. No Al solubility was found in U_2Ti phase at either temperature.

Acknowledgement

The authors thank F. Gouttefeangeas and L. Joanny at the Centre de Microscopie Électronique à Balayage et microAnalyse (CMEBA) for the SEM-EDS analyses. We also thank T. Roisnel and V. Dorcet at Centre de Diffraction X (CDIFX) for the single crystal data collection.

References

[1] V. Sechovsky, G. Hilscher, Physica B., 130 (1985) 207.

[2] A. Zentko, J. Hřebík, J. Šternberk, J. Turán, Physica B, 102 (1980) 269.

[3] A. Periccone, H. Noël, J. Nucl. Mater., 299 (2001) 260.

[4] O. Eriksson, B. Johansson, H.L. Skriver, M.S.S. Brooks, Physica B, 144 (1986) 32.

[5] M.S.S. Brooks, O. Eriksson, B. Johansson, J.J.M. Franse, P.H. Frings, J. Phys. F.: Met. Phys., 18 (1988) L33.

[6] P. Boulet, G.M. Gross, G. André, F. Bourée, H. Noël, J. Solid State Chem., 144, (1999) 311.

[7] A. Mar, O. Tougait, M. Potel, H. Noël, E.B Lopes, Chem. Mater., 18, (2006) 4533

[8] L. Havela, V. Sechovsky, J. Hrebik, A.V. Andreev, J. Less Comm. Met., 114 (1985) 317.

[9] S. Niemann, W. Jeitschko, J. Solid State Chem. 114, (1995) 337

[10] Y. Matsumoto, T.D. Matsuda, N. Tateiwa, E. Yamamoto, Y. Haga, Z. Fisk, J. Korean Phys. Soc., 63 (2013) 363.

[11] A. Leenaers, S. Van den Berghe, E. Koonen, C. Jarousse, F. Huet, M. Trotabas, M. Boyard, S. Guillot, L. Sannen, M. Verwerft, J.Nucl. Mater., 335, (2004) 39.

[12] Y.S Kim, G.L. Hofman, A.B. Robinson, D.M. Wachs, H.J. Ryu, J.M. Park, J.H. Yang, J. Nucl. Mater. 427 (2012) 233.

[13] J. Allenou, H. Palancher, X. Iltis, O. Tougait, H. El Bekkachi, A. Bonnin, R. Tucoulou, J. Nucl. Mater. 446 (2014) 208.

[14] H. Noël, O. Tougait, S. Dubois, J. Nucl. Mater., 389 (2009) 93

[15] Brüker-AXS, In: Collect, Denzo, Scalepack, Sortav. Kappa CCD Program Package, Delft, The Netherlands, 1998.

[16] J. de Meulenaer, H. Tompa, *Acta Crystallogr. Sect. A 19*, (1965**)** 1014.

[17] G. M. Sheldrick, Acta Crystallogr., Sect A, 64 (2008) 112.

[18] T.B. Massalski, H. Okamoto, P.R. Subramanian, L. Kacprzak (Eds.), Binary Alloy Phase Diagrams, vols. 1–3, second ed., ASM International, 1990.

[19] F. Zhang, S.L. Chen, Y.A. Chang, U.R. Kattner, Intermetallics 5 (1997) 471.

[20] I. Ohnuma, Y. Fujita, H. Mitsui, K. Ishikawa, R. Kainuma, K. Ishida, Acta mater. 48 (2000) 3113.

[21] F.H. Ellinger, R.O. Elliott, E.M. Cramer, J. Nucl. Mater., 1 (1959) 233

[22] C.W. Tucker Jr., P. Senio, Acta Crystallogr., 6 (1953) 753.

[23] A.S. Wilson, R.E. Rundle, Acta Crystallogr., 2 (1949) 126.

[24] P. Ehrlich, Z. Anorg. Chem., 259 (1949), 1

[25] A. Taylor, R.W. Floyd, J. Inst. Met., 80 (1951/52), 577.

[26] G. Grube, L. Botzenhardt, Z. Elektrochem. Angew. Phys. Chem., 48 (1942) 418.
[27] A.G. Knapton, Acta Crystallogr., 7 (1954) 457.
[28] E. Ence, H. Margolin, Trans. Am. Inst. Min. Metall. Pet. Eng., 209 (1957) 484.
[29] P.E. Duwez, J.L. Taylor, Trans. Am. Inst. Min. Metall. Pet. Eng., 194 (1952) 70.
[30] K. Schubert, H.G. Meissner, M. Poetzschke, W. Rossteutscher, E. Stolz, Naturwissenschaften, 49 (1962) 57.
[31] K. Schubert, H.G. Meissner, A. Raman, W. Rossteutscher, Naturwissenschaften, 51 (1964) 287.
[32] A. Raman, K. Schubert, Z. Metallkd., 56 (1965) 44.
[33] S. Steeb, G. Petzow. Naturwissenschaften, 48 (1961) 450.
[34] O. Tougait, H. Noël, Intermetallics 12 (2004) 219
[35] E. Teatum, K. Gschneidner, J. Waber, LA-2345 Los Alamos Scientific Laboratory (1960)

TABLE 1. Crystallographic data and stability domain of the binary boundary phases of the U-Ti-A system.

Phase	Structure type	Space group	Lattice parameters (Å)			Domain of stability (K)	Composition range (1123K)	Composition range (923K)	ref
αU	αU	*Cmcm*	2.8542	5.8667	4.9540	< 941			21
βU	βU	$P4_2/mnm$	10.7590	10.7590	5.6560	941-1049			22
γU		$Im\bar{3}m$	3.4900	3.4900	3.4900	1049-1408	2 at.% Al 15 at.% Ti	0 at.% Al 2 at.% Ti	23
αTi	Mg	$P6_3/mmc$	2.9490	2.9490	4.7270	<1155	15 at.% Al	12.5 at.% Al 1 at.% U	24
βTi	W	$Im\bar{3}m$	3.3300	3.3300	3.3300	1155-1943	2-34 at.% U		25
Al	Cu	$Fm\bar{3}m$	4.0410	4.0410	4.0410	<933			26
U_2Ti	Hg_2U	*P6/mmm*	4.8280	4.8280	2.8470	<1171			27
Ti_3Al	Mg_3Cd	$P6_3/mmc$	5.77500	5.7750	4.6380	<1455	22-36 at.% Al	22-35 at.% Al	28
TiAl	CuAu	*P4/mmm*	4.0040	4.0040	4.0710	<1753	49-57 at.%	49-56 at.%	29
$TiAl_2$	$HfGa_2$	$I4_1/amd$	3.9760	3.9760	24.3600	<1513	65-66 at.%	65-65.4 at.%	30
$Ti_{1.25}Al_{2.75}$	$Ti(Ti_{0.25}Al_{0.75})Al_2$	*I4/mmm*	3.9170	3.9170	16.5240	1423-1653			31
$TiAl_3$	$TiAl_3$	*I4/mmm*	3.8400	3.8400	8.5800	<1623			32
UAl_2	$MgCu_2$	$Fd\bar{3}m$	7.7763	7.7763	7.7763	<1893			33
UAl_3	Cu_3Au	$Fm\bar{3}m$	4.2660	4.2660	4.2660	<1623			34
UAl_4	UAl_4	*Imma*	4.4014	6.2552	13.7279	<1004			34

TABLE 2. Compositions (in at. %) of phases obtained for samples heat-treated at 923K

Nominal sample composition	Phase field	Phase composition determined by MEB-EDS (at.%)		
8U-4Ti-88Al	(Al)+(UTi_2Al_{20})+(UAl_4)	(Al): 100(1)Al	(UTi_2Al_{20}): 5(1)U-8(1)Ti-87(1)Al	(UAl_4): 20(1)U-80(1)Al
2U-9Ti-89Al	(Al)+(UTi_2Al_{20})+($TiAl_3$)	(Al): 100(1)Al	(UTi_2Al_{20}): 4(1)U-9(1)Ti-87(1)Al	($TiAl_3$): 25(1)Ti-75(1)Al
11.32U-7.55Ti-81.13Al	(UAl_3)+(UTi_2Al_{20})+($TiAl_3$)	(UAl_3): 25(1)U-75(1)Al	(UTi_2Al_{20}): 4(1)U-9(1)Ti-87(1)Al	($TiAl_3$): 24(1)Ti-76(1)Al
24U-5Ti-71Al	(UAl_3)+($TiAl_3$)+(UAl_2)	(UAl_3): 25(1)U-75(1)Al	($TiAl_3$): 25(1)Ti-75(1)Al	(UAl_2): 33(1)U-66(1)Al-1(1)Ti
16.67U-16.67Ti-66.67Al	(UAl_2)+($TiAl_2$)	(UAl_2): 33(1)U-67(1)Al	($TiAl_2$): 33(1)Ti-67(1)Al	
33U-22Ti-45Al	(UAl_2)+(TiAl)+(U)	($UAl_{2-x}Ti_x$): 33(1)U-62(1)Al-5(1)Ti	(TiAl): 50(1)Ti-50(1)Al	(U): NA*
50U-20Ti-30Al	(UAl_2)+(TiAl)+(U)	($UAl_{2-x}Ti_x$): 34(1)U-61(1)Al-5(1)Ti	(TiAl): 51(1)Ti-49(1)Al	(U): 100(1)U
38U-5Ti-Al57	(U) + UAl_2	(U): 100(1)U	($UAl_{2-x}Ti_x$): 33(1)U-62(1)Al-5(1)Ti	
33.3U-33.3Ti-33.3Al	(U) + (TiAl)	(U): 98(1)U-2(1)Ti	(TiAl): 50(1)Ti-50(1)Al	
60U-20Ti-20Al	(U) + (TiAl)	(U): 100(1)U	(TiAl): 51(1)Ti-49(1)Al	
40U-40Ti-20Al	(Ti_3Al)+(U)	(Ti_3Al): 66(1)Ti-34(1)Al	(U): 98(1)U-2(1)Ti	
65U-30Ti-5Al	(Ti_3Al)+(U)+(U_2Ti)	(Ti_3Al): 73(1)Ti-27(1)Al	(U): 98(1)U-2(1)Ti	(U_2Ti): 67(1)U-33(1)Ti
20U-60Ti-20Al	(Ti_3Al)+(U_2Ti)	(Ti_3Al): 74(1)Ti-26(1)Al	(U_2Ti): 67(1)U-33(1)Ti	
10U-80Ti-10Al	(αTi)+(U_2Ti)	(αTi): 87(1)Ti-13(1)Al	(U_2Ti): 67(1)U-33(1)Ti	

*NA: not accurate due to too small size grains.

TABLE 3. Compositions (in at. %) of phases obtained for samples heat-treated at 1123K

Nominal sample composition	Phase field	Phase composition determined by MEB-EDS		
8U-4Ti-88Al	(Al)+(UTi_2Al_{20})+(UAl_3)	(Al): 98(1)Al-1(1)U-1(1)Ti	(UTi_2Al_{20}): 5(1)U-9(1)Ti-86(1)Al	(UAl_3): 25(1)U-75(1)Al
2U-9Ti-89Al	(Al)+(UTi_2Al_{20})+($TiAl_3$)	(Al): 99(1)Al-1(1)U	(UTi_2Al_{20}): 4(1)U-9(1)Ti-87(1)Al	($TiAl_3$): 25(1)Ti-75(1)Al
10U-10Ti-80Al	(UAl_3)+(UTi_2Al_{20})+($TiAl_3$)	(UAl_3): 25(1)U-75(1)Al	(UTi_2Al_{20}): 5(1)U-9(1)Ti-86(1)Al	($TiAl_3$): 24(1)U-76(1)Al
24U-5Ti-71Al	(UAl_3)+($TiAl_3$)+(UAl_2)]	(UAl_3): 25(1)U-75(1)Al	($TiAl_3$): 25(1)Ti-75(1)Al	(UAl_2): 33(1)Ti-67(1)Al
20U-10Ti-70Al	(UAl_2)+($TiAl_2$)	(UAl_2): 33(1)U-67(1)Al	($TiAl_2$): 34(1)Ti-66(1)Al	
33U-22Ti-45Al	(U) + (UAl_2)+(TiAl)	(U): 96(1)U-2(1)Ti-2(1)Al	(UAl_2): 33(1)U-5(1)Ti-62(1)Al	(TiAl): 51(1)Ti-49(1)Al
50U-20Ti-30Al	(U) + (UAl_2)+(TiAl)	(U): 96(1)U-2(1)Ti-2(1)Al	(UAl_2): 33(1)U-6(1)Ti-61(1)Al)	(TiAl): 52(1)Ti-48(1)Al
40U-10Ti-50Al	(U) + (UAl_2)+(TiAl)	(U): 96(1)U-2(1)Ti-2(1)Al	(UAl_2): 33(1)U-5(1)Ti-62(1)Al	(TiAl): 51(1)Ti-49(1)Al
16.67U-16.67Ti-66.67Al	(UAl_2)+($TiAl_2$)	(UAl_2): 31(1)U-3(1)Ti-66(1)Al	($TiAl_2$): 33(1)Ti-67(1)Al	
60U-20Ti-20Al	(U) + (TiAl)	(U): 96(1)U-2(1)Ti-2(1)Al	(TiAl): 51(1)Ti-49(1)Al	
70U-28Ti-2Al	(U) + (U_2Ti) + (Ti_3Al)	(U): 84(1)U-16(1)Ti	(U_2Ti): 67(1)U-33(1)Ti	(Ti_3Al): 33(1)Ti-67(1)Al
10U-80Ti-10Al	(U_2Ti) + (βTi) + (αTi)	(U_2Ti): 67(1)U-33(1)Ti	(βTi): 14(1)U-80(1)Ti-6(1)Al	(αTi) : 86(1)Ti-14(1)Al
16U-80Ti-4Al	(βTi) + (αTi)	(βTi): 17(1) U-79(1)Ti-4(1)Al	(αTi) : 89(1)Ti-11(1)Al	

TABLE 4. Crystal data and structure refinement parameters for UTi_2Al_{20}

Chemical formula	$UTi_{2.}Al_{20}$
Formula weight ($g.mol^{-1}$)	873.4
Crystal system, space group	cubic, $Fm\bar{3}d$ (# 227)
Unit cell dimensions (Å)	a = 14.634(1)
Volume ($Å^3$)	3133.7(1)
Z, Calculated density (g/cm^3)	8, 3.70
Absorption coefficient (cm^{-1})	124.1
Crystal color and habit	Black, coffin like
Crystal size (mm^3)	0.15 x 0.07 x 0.05
Theta range for data collection (°)	2.41 to 45.14
Limiting indices	-29≤h≤28, -28≤k≤29, -29 ≤ l ≤ 28
Reflections collected / unique	21188 / 674
R(int)	0.115
Absorption correction	Analytical
Data / restraints / parameters	605 / 0 / 18
Goodness-of-fit on F^2	1.24
R indices* [I>2σ(I)]	R_1 = 0.0280, wR_2 = 0.071
Extinction coefficient	0.00334(18)
Largest diff. peak and hole ($e.Å^{-3}$)	3.55 and -3.74
$* R(F) = \sum \lVert F_0 \rvert - \lvert F_C \rVert / \lvert F_C \rvert$ (for $F^2>2\sigma(F^2)$)	
$wR_2 = \left[\sum w(F_o^2-F_c^2)^2 / wF_o^4\right]^{½}$, where $w^{-1} = [\sigma^2(F_o^2) + (Ap)^2 + Bp]$, $p = [\max(F_o^2,0) + 2F_c^2]/3$	

TABLE 5. Atomic coordinates and equivalent isotropic displacement parameters (Å^2) for UTi_2Al_{20}.

Atom	Wyckoff position	x	y	z	U_{eq}. (Å^2)
U(1)	8a	$^1/_8$	$^1/_8$	$^1/_8$	0.0096(1)
Ti(1)	16d	½	½	½	0.0071(2)
Al(1)	16c	0	0	0	0.0164(4)
Al(2)	48f	0.48726(9)	$^1/_8$	$^1/_8$	0.0097(2)
Al(3)	96g	0.05994(4)	0.05994(4)	0.32344(6)	0.0121(2)

U_{eq} is defined as one third of the trace of the orthogonalized Uij tensor.

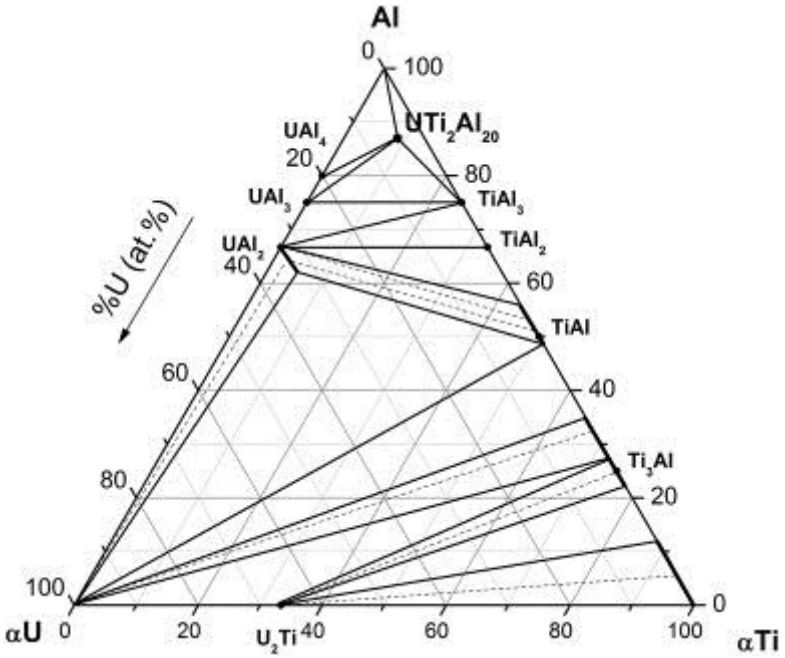

Figure.1: Phase relations in the ternary U-Ti-Al system, constructed from samples heat-treated at 923K

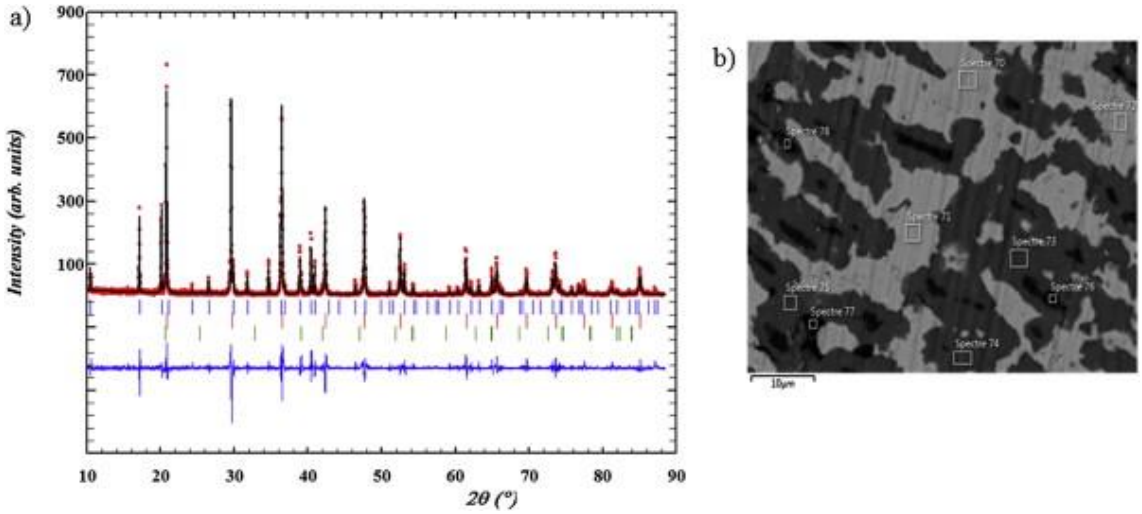

Figure 2: (a) Experimental XRD pattern (red symbols) of sample with composition 11.32U-7.55Ti-81.13Al annealed at 923 K for 720h and calculated (black line) profile using the Le Bail method. The theoretical positions of the phases in presence are plotted as vertical ticks: UTi_2Al_{20} (upper blue), UAl_3 (middle red) and $TiAl_3$ (lower green). The difference line between experimental and calculated patterns is plotted on the lower blue curve. (b) Corresponding SEM image in backscattered electron mode showing the presence of UTi_2Al_{20} (medium grey), UAl_3 (light grey) and $TiAl_3$ (black).

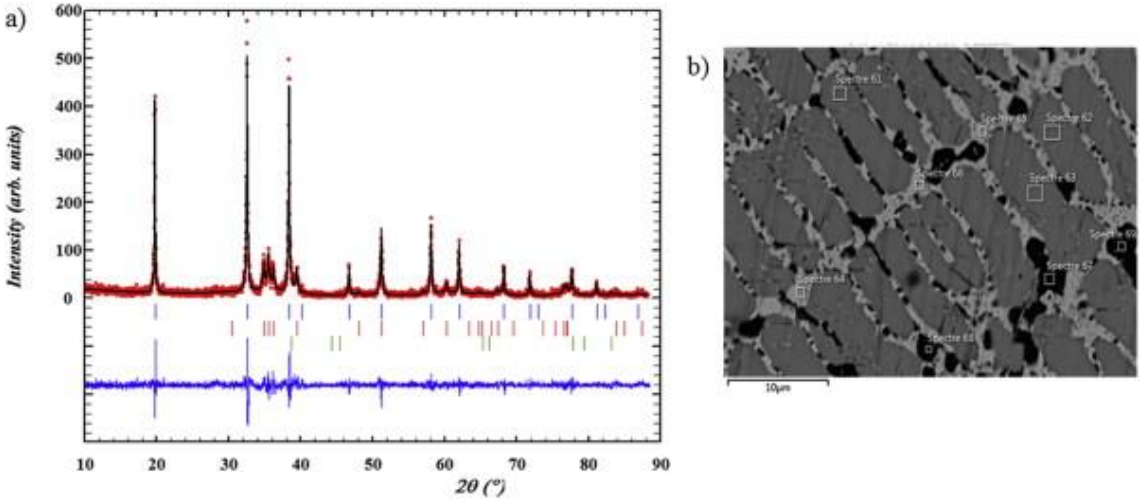

Figure 3: (a) Experimental XRD pattern (red symbols) of sample with composition 40U-40Ti-20Al annealed at 923 K for 720h and calculated (black line) profile using the Le Bail method. The theoretical positions of the phases in presence are plotted as vertical ticks: $UAl_{2-x}Ti_x$, x = 0.05 (upper blue), αU (middle red) and TiAl (lower green). The difference line between experimental and calculated patterns is plotted on the lower blue curve. (b) Corresponding SEM image in backscattered electron mode showing the presence of: $UAl_{2-x}Ti_x$, x = 0.05 (medium grey), αU (light grey) and TiAl (black).

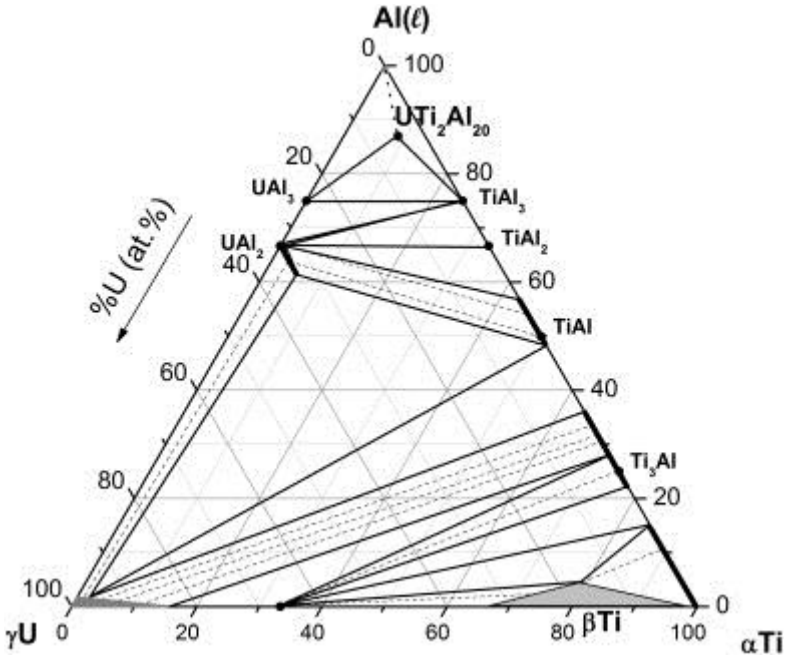

Figure.4: Phase relations in the ternary U-Ti-Al system, constructed from samples heat-treated at 1123K. The dotted line corresponds to the equilibrium with the melt in the Al-rich part.

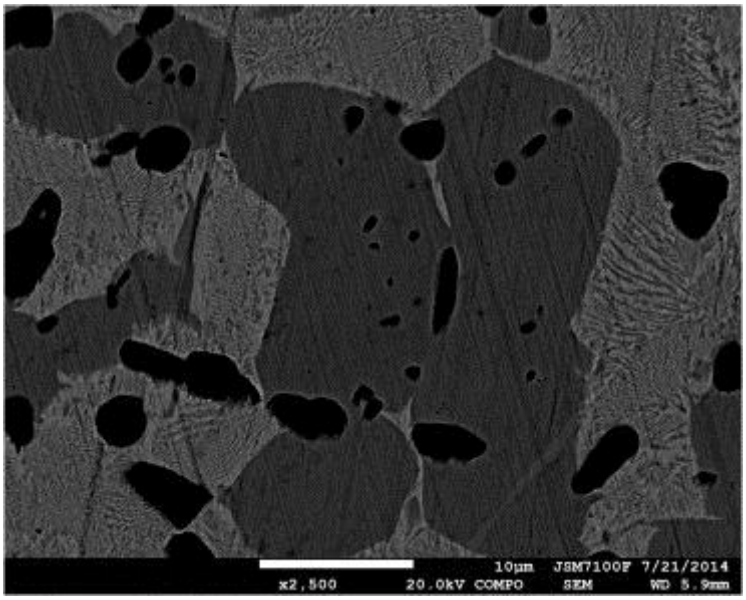

Figure 5: backscattered image of a sample 70U-28Ti-2Al, the black grains correspond to Ti_3Al, the grey grains to U_2Ti and the lamellar morphology of U featuring a rapid decomposition.